

Synthesis and characterization of cerium doped yttrium-gadolinium aluminate phosphors by wet-chemical synthesis route

E. J. POPOVICI^{a*}, M. MORAR^b, E. BICA^a, I. PERHAITA^a, A. I. CADIS^a, E. INDREA^c,
L. BARBU-TUDORAN^d

^aRaluca Ripan Institute for Research in Chemistry, Babes-Bolyai University Cluj-Napoca, 400294 Cluj-Napoca, Romania

^bTechnical University of Cluj-Napoca, 400114 Cluj-Napoca, Romania

^cNational Institute for Research and Development of Isotopic and Molecular Technologies,
400293 Cluj-Napoca, Romania

^dElectronic Microscopy Centre, Babes-Bolyai University Cluj-Napoca, 400006 Cluj-Napoca, Romania

Synthesis of cerium activated yttrium gadolinium aluminate phosphors (Y,Gd)₃Al₅O₁₂:Ce using the wet-chemical synthesis route via the reagent simultaneous addition technique (WCS-SimAdd) is reported for the first time. Y-Gd-Ce-Al precursors with variable Y:Gd ratios have been precipitated from metal nitrates and urea solutions that were simultaneously added, in an aqueous medium with controlled pH and temperature. The precursor nanopowders were intimately mixed with NH₄Cl (flux) and calcined for 2 hrs at 1200°C, in nitrogen flow and converted into micro-powders of phosphor with nominal formula Y_{2.97-x}Gd_xCe_{0.03}Al₅O₁₂ (where x=0; 0.75; 1.50; 2.25; 2.97). Chemical composition and thermal behaviour of precursors as well as the PL properties, and morphological and structural characteristics of phosphor powders were investigated in relation with the Gd amount. WCS-SimAdd route enables a good control of the synthesis conditions to prepare (Y,Gd)₃Al₅O₁₂:Ce³⁺ phosphors with cubic/garnet crystalline structure, regular particle dimensions and shapes and intense yellow-to-orange emission appropriate for use in LED type optoelectronic devices.

(Received May 5, 2011; accepted June 9, 2011)

Keywords: Phosphors; Chemical synthesis; Luminescence; X-ray diffraction; Scanning electron microscopy

1. Introduction

White light emitting diodes (WLEDs), the so-called next generation solid-state lighting sources, are gaining lots of attention because of their numerous advantages over the existing incandescent and fluorescent lamps in relation with the energy saving, reliability, lifetime and environmental-amity [1]. Although the white radiation can be generated with many methods, the combination of GaN-based blue LED and cerium-activated yttrium aluminium garnet Y₃Al₅O₁₂:Ce³⁺ (YAG:Ce) phosphor is the most popular and sophisticated method at present [2]. YAG:Ce phosphor has been found to be suitable for converting the blue LED radiation into a very broad band yellow emission. In the same time, YAG:Ce phosphor has a broad excitation band and this provides a basis for its use along with GaN LEDs to produce white light [3,4].

More than that, there is a large variety of LEDs based on chips with variable blue light wavelength peaking from 450 to 480 nm. For this reason, it is necessary to prepare YAG:Ce type phosphors with adjustable wavelength matching the blue LEDs, in order to obtain ideal white light [5]. However, this strategy based on YAG:Ce phosphors suffers from low colour-rendering index and high colour-temperature, due to the weak emission intensity in red spectral region. The colour balance can be improved either by adding some red-emitting components

into YAG:Ce phosphor, or by doping the garnet lattice with desirable cations to slightly adjust the luminescence colour [6,7].

The emission wavelength of Y₃Al₅O₁₂:Ce³⁺ phosphors can be tuned by partially or totally substituting Y³⁺ with Gd³⁺ in the YAG:Ce garnet structure, to obtain cerium doped yttrium-gadolinium aluminium garnet (Y_{1-x}Gd_x)₃Al₅O₁₂:Ce³⁺ (hereinafter YGAG:Ce) and, at limit, Gd₃Al₅O₁₂:Ce³⁺ compound (hereinafter GAG:Ce).

It is known that there are three stable phases in the Y₂O₃-Al₂O₃ or Gd₂O₃-Al₂O₃ pseudo-binary systems i.e. hexagonal, perovskite YAIO₃ or GdAlO₃ (YAP or GAP), monoclinic Y₄Al₂O₉ or Gd₄Al₂O₉ (YAM or GAM), and cubic, garnet Y₃Al₅O₁₂ or Gd₃Al₅O₁₂ (YAG or GAG) [8,9]. Among them, only YAG and GAG phases are effective as host lattice for rare earth activated phosphors.

YGAG:Ce and GAG:Ce phosphors can be prepared by a variety of methods, starting with the classic solid state reaction (SSR) route that requires high temperature sintering with repeated grinding and milling. (Y, Gd)Al₅O₁₂:Ce³⁺ garnets can be obtained by SSR route at 1400-1550°C, for 3- 6 hrs, in reducing atmosphere [1,7]. The sintering temperature can be efficiently decreased using alternative methods such as wet-chemical synthesis route/co-precipitation [10], sol-gel [11, 12], combustion [13, 14], solvothermal [15, 16], glycothermal [17], polyesterification [18], etc.

Synthesis of $(Y_{1-x}Gd_x)_3Al_5O_{12}: Ce^{3+}$ phosphors with pure cubic, garnet structure is rather difficult [10]. Because garnets are mixed oxides with a definite stoichiometry, the synthesis strategy used for their preparation is intrinsically more complex and delicate than for simple oxides such as Y_2O_3 [19]. One can also note that, there are few reports referring to the synthesis of $(Y,Gd)_3Al_5O_{12}: Ce^{3+}$ phosphors by WCS co-precipitation route, probable in correlation with the difficulties to control the phosphor composition.

The goal of our studies is the synthesis of fine powders of cerium-doped yttrium-gadolinium aluminium garnets with good photoluminescence performances, utilisable in white LED manufacture. In this respect, attempts were made to use and develop the WCS route based on the reagents simultaneous addition technique WCS-SimAdd, which we have successfully used for the manufacture of yttrium oxide-based phosphors [20-22]. It is the aim of this work to explore the possibility of preparing pure $(Y,Gd)_3Al_5O_{12}: Ce^{3+}$ garnet micro powders, using the WCS-SimAdd route. With this purpose in mind, the photoluminescence properties as well as the morphological and structural characteristics of $(Y,Gd)_3Al_5O_{12}: Ce^{3+}$ phosphors were investigated in correlation with gadolinium concentration.

2. Experimental part

2.1. Sample preparation

Phosphors $(Y_{1-x}Gd_x)_3Al_5O_{12}: Ce^{3+}$ were prepared by thermal synthesis, from Y-Gd-Al-Ce precursors obtained by wet-chemical synthesis route *via* the reagent simultaneous addition technique. Two $(Y,Gd)_3Al_5O_{12}: Ce^{3+}$ sample series with 0; 25; 50; 75 and 100 mol% gadolinium were synthesised with or without NH_4Cl as flux, in order to prepare YAG:Ce, YGAG:Ce and GAG:Ce phosphors.

Phosphor samples with general formula $Y_{2.97-x}Gd_x Ce_{0.03} Al_5O_{12}$, where $x=0; 0.75; 1.50; 2.25; 2.97$ were synthesised from Y-Gd-Al-Ce precursors prepared by WCS-SimAdd technique, from metal nitrates and urea. The starting materials were Y_2O_3 (99.9%; Fluka), Gd_2O_3 (99+, Merck); $Al(NO_3)_3 \cdot 9H_2O$ (98%; Alfa Aesar), $Ce(NO_3)_3 \cdot 6H_2O$ (extrapure; Merck) as metallic ion source and urea H_4CN_2O (ACS, AlphaAesar), as anion source. Prior use, yttrium and gadolinium oxides were dissolved in small amount of HNO_3 ($d=1.42$; Merck). The precipitation was carried out at $80^\circ C$, under constant stirring and pH. In this respect, equal volumes of metal (III) nitrate mixture solution and, correspondingly, urea in 1:4 molar ratio, were simultaneously added, with controlled flow, into urea diluted solution [20-24]. The nitrate mixture contains stoichiometric amounts of Y^{3+} , Gd^{3+} , Ce^{3+} and Al^{3+} corresponding to the molar ratio (Y+Gd): Ce: Al = 2.97: 0.03: 5. After the aging period, the precipitates were water washed, centrifuged, dried and crushed.

The thermal synthesis of phosphors was performed without or with NH_4Cl as flux, at $1200^\circ C$, in N_2 atmosphere. YAG: Ce, YGAG:Ce and GAG:Ce powders

were water washed, dried and sieved. No ball milling was used during the phosphor processing.

2.2. Samples investigation

Precursors and phosphors were characterised by *photoluminescence measurements* (JASCO FP-6500 Spectrofluorimeter Wavel; Glass filter WG 320), *X-ray diffraction* (BRUKER D8 Advance X-ray diffractometer, $CuK\alpha_1$), *thermal analysis* (Mettler Toledo TGA/SDTA851 thermogravimetric cell), *FTIR spectral analysis for gases evolved during the thermal analysis* (Thermo Scientific Nicolet 6700 FT-IR Spectrometer, equipped with TGA Module), *chemical analysis* (Perkin Elmer, ICP-OES spectrometer OPTIMA 2100 DV) and *scanning electron microscopy* (JEOL –JSM 5510LV Microscope; Au coated samples).

3. Results and discussion

Cerium doped yttrium-gadolinium aluminium garnets were prepared by thermal synthesis, with NH_4Cl as flux, from precursors obtained by WCS-SimAdd route, from metal(III) nitrates and urea as homogeneous precipitant. Properties of $(Y,Gd)_3Al_5O_{12}: Ce^{3+}$ phosphors depend on the quality of Y-Gd-Ce-Al precursors precipitated on the basis of urea hydrolysis. It is known that urea hydrolysis is a mild process, and urea has been used as the ligand source for ammonia in a traditional homogeneous precipitation method [25]. The active release of OH^- and CO_3^{2-} ions, usually leads to the precipitation of metal hydrous oxide particles [26]. In multi-component system, such as Y^{3+} - Gd^{3+} - Ce^{3+} - Al^{3+} nitrate, the chemical composition of the multi-metal hydrous oxides as well as the precursor characteristics i.e. particle shape and size, specific surface area and porosity, reactivity are quite sensitive towards pH, metal ion concentration, temperature and aging time.

Synthesis of $(Y,Gd)_3Al_5O_{12}: Ce^{3+}$ phosphors is based on homogeneous precipitation of precursors, with the mention that the two reagent solutions Y^{3+} , Gd^{3+} , Ce^{3+} and Al^{3+} nitrate mixture and correspondingly, urea are simultaneously added, with constant, low flow, into a diluted urea solution. In these conditions, the precipitation produces in an environment with no concentration or pH gradient, thus enabling a good control of the Y-Gd-Al precursor quality.

Phosphors with nominal formula $Y_{2.97-x}Gd_x Ce_{0.03} Al_5O_{12}$ (where $x=0; 0.75; 1.5; 2.25; 2.97$) were investigated in relation with their morphological and structural characteristics as well as the photoluminescence properties, in dependence on the gadolinium content.

3.1. Physical-chemical characteristics of Y-Gd-Ce-Al precursors

Yttrium, gadolinium, cerium and aluminium ions interact with hydrolysis products of urea to form highly dispersed homogeneous, white powders of precursors, with well defined composition. Due to the complexity of

the simultaneous process of precipitation of Y^{3+} , Gd^{3+} , Ce^{3+} and Al^{3+} oxide compounds, the precursors were monitored in relation with both the anionic and cationic composition.

The thermogravimetric measurements, coupled with FTIR absorption spectroscopic investigation of the evolved gases, were used to determine the anionic composition of precursors whereas the actual molar ratio between the metals was determined by inductive plasma coupled optical emission spectroscopy (ICP-OES).

The thermogravimetric curves (TGA) illustrate that Y-Gd-Ce-Al precursors decompose in five major steps, with

a total weight loss (Δ_{1100}) that monotonously decreases from 45.2 wt% for Y-Ce-Al precursor to 34.2 wt%, for Gd-Ce-Al precursor (Table 1). According to the differential thermal analysis curves (SDTA), all the decomposition processes were endothermic. Beside them, a relative strong exothermic process was noticed, in relation with the formation/crystallization of yttrium-gadolinium aluminate lattice. The temperature T_{exo} of this characteristic exo-effect decreases monotonously with the increase of Gd amount, from 925 °C for Y-Ce-Al precursor to 910°C for Gd-Ce-Al precursor.

Table 1. Composition of $Y_{2.97-x}Gd_xCe_{0.03}Al_5O_{12}$ phosphors and the thermal analysis characteristics of the corresponding precursors

N r.	Phosphor formula	Rare earth atomic ratios (RE/ Σ RE)						TGA/SDTA	
		Theoretic(mol%)			Experimental (mol%)			Δ_{1100} (wt%)	T_{cryst} (°C)
		Gd	Y	Ce	Gd	Y	Ce		
1.	$Y_{2.97}Ce_{0.03}Al_5O_{12}$	0	99.00	1	0	99.03	0.97	45.2	925
2.	$Y_{2.22}Gd_{0.75}Ce_{0.03}Al_5O_{12}$	24.00	75.00	1	24.39	74.74	0.87	42.1	923
3.	$Y_{1.47}Gd_{1.5}Ce_{0.03}Al_5O_{12}$	49.00	50.00	1	49.79	49.45	0.76	44.0	921
4.	$Y_{0.72}Gd_{2.25}Ce_{0.03}Al_5O_{12}$	74.00	25.00	1	75.80	23.47	0.74	38.0	918
5.	$Gd_{2.97}Ce_{0.03}Al_5O_{12}$	99.00	0	1	99.30	0	0.70	34.2	910

Y-Gd-Al-Ce precursors can be considered as mixtures of metal (III) hydroxides, hydrogen carbonates and nitrates, with small amounts of slightly bounded ammonia and water. According to TGA-FTIR data, Y-Gd-Ce-Al precursors can be expressed by the general formula $xM(OH)_3 \cdot yM(HCO_3)_3 \cdot zM(NO_3)_3 \cdot vNH_3 \cdot wH_2O$ where the x:y:z:v:w is variable, depending on the initial Y:Gd ratio.

The actual Gd:Y ratio in precursors is very close to the theoretical value (Table 1) Opposite situation is observed for Ce-amount. In our experimental conditions, the co-precipitation level of Ce^{3+} ions decreases from 97% in Y-Ce-Al-precursor to 70% in Gd-Ce-Al-precursor. This tendency can be partially explained by the differences between the solubility product values. If one considers that precursors are simply formed from metallic hydroxides, the solubility product constants expressed by pK_{sp} (at 25°C) vary in the order: 32.89, for $Al(OH)_3$ > 22.74, for $Gd(OH)_3$ > 22.00, for $Y(OH)_3$, > 19.80, for $Ce(OH)_3$ respectively [27]. According to pK_{sp} values, the precipitation rate of hydroxides varies in the same order $Al > Gd > Y > Ce$ and this could explain the tendency of cerium hydroxide to precipitate relative slower, so that the actual Ce^{3+} -doping level decrease monotonously with Gd amount.

For WCS methods, the synthesis conditions are extremely important for the physical-chemical characteristics of precursors that directly determine the phosphors composition and therefore, their properties. In the present case, the aluminium hydroxide is amphoteric, and the precipitation level of aluminium into the multi-component precursor depends strongly on the precipitation/maturation pH. The solubility of aluminium hydroxide is minimum at pH = 7.7 corresponding to the isoelectric point [28]. In our experiments, the WCS-

SimAdd synthesis conditions enable a molar ratio $Al_2O_3:Re_2O_3$ close to the theoretical value 1.66.

3.2. Morphological and structural properties

Cerium-doped yttrium-gadolinium aluminium garnet samples are yellow-to-orange, polycrystalline powders, depending on gadolinium content. According to XRD patterns, all precursors are amorphous powders whereas all phosphors are homogeneous, crystalline materials with cubic garnet type structure (Fig. 1). The phosphor powders obtained by WCS-SimAdd contain no impurity phases such as unreacted yttria or alumina and other aluminate phases viz. YAM/GAM; YAP/GAP. Although the synthesis was performed in a single, short stage, at relatively low temperature (1200°C), the good quality of precursors results in well crystallized homogeneous materials, with cubic structure; this is contrary to our expectation, for the $GdAlO_3$ formation has been frequently reported [1, 6, 29].

The experimental and Rietveld fitted XRD patterns of samples show the evidence of the cubic aluminium garnet crystal structure, $Y_3Al_5O_{12}:Ce$ the space group Ia-3d (SG 230) [30] The measured peak positions are in good agreement with Rietveld fitting and data given in Powder Diffraction Files for $Y_3Al_5O_{12}$ (PDF 79–1892) and $Gd_3Al_5O_{12}$ (PDF 73 – 1371). Rietveld analysis based on pseudo-Voigt profile fitting function was applied to perform a simultaneous refinement of X-ray diffraction patterns concerning both material structure and microstructure [31]. The unit cell parameters, the effective crystallite mean size, D_{eff} (nm) and the root mean square (rms) of the microstrains $\langle \epsilon^2 \rangle_m^{1/2}$ were determined, using the PowderCell software [32, 33].

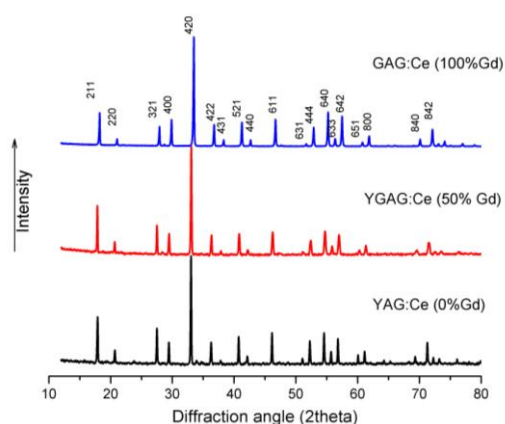


Fig. 1. X-ray diffraction patterns of $Y_{2.97-x}Gd_xCe_{0.03}Al_5O_{12}$ samples ($x=0; 1.50; 2.97$).

In $(Y,Gd)_3Al_5O_{12}$ polycrystalline powders, the unit cell parameter a (nm) for the garnet phase increases linearly with Gd concentration, from 1.2017 nm for 0 mol% Gd^{3+} to 1.2106 nm for 100 mol% Gd^{3+} (Fig.2a). The experimental values are in agreement with the literature data i.e. $a=1.2016$ nm for $Y_3Al_5O_{12}$ (PDF 79-1892) and $a=1.2113$ nm for $Gd_3Al_5O_{12}$ (PDF 73-1371). Due to the very close crystal radii values, the partial or total substitution of Y^{3+} ($r = 0.104$ nm) with Gd^{3+} ($r = 0.108$ nm) ions into $Y_3Al_5O_{12}$ crystal brings about the formation of the solid solution dominated by Vegard's rule. Accordingly, the crystal parameters vary linearly with the molar concentration of the substituting ions. The rather good linear fitting of the dependence of the unit cell parameter on Gd concentration proves that the WCS-SimAdd route enables a good control of the crystalline phase composition of $(Y,Gd)_3Al_5O_{12}$ phosphors.

Mention has to be made that, $(Y,Gd)_3Al_5O_{12} :Ce^{3+}$ powders are garnet solid solutions in the system $Y_3Al_5O_{12} - Gd_3Al_5O_{12}$, where part of Y^{3+}/Gd^{3+} ions are substituted by the activator ions, Ce^{3+} . Although Ce^{3+} ions are relative larger ($r=0.115$ nm) than the substituted ions, the activator concentration (1 mol% from the total rare earth ions positions) is too small to affect the crystalline parameters. The dependence of the crystallite size D_{eff} and the root mean square of microstrain $\langle \varepsilon^2 \rangle_m^{1/2}$ of $(Y,Gd)_3Al_5O_{12}$ garnet phase versus the gadolinium concentration is depicted in Fig.2b).

The microstructural parameters of Ce-doped $(Y,Gd)_3Al_5O_{12}$ phosphors show that, as Gd concentration increases, the average size of the particles decreases from 93 nm for samples without gadolinium ($Y_3Al_5O_{12}$) to 24 nm for sample with 75 mol% Gd, and then increases abruptly to about 97 nm, for $Gd_3Al_5O_{12}$. In the same time, the lattice microstrain $\langle \varepsilon^2 \rangle_m^{1/2}$ increases slowly from 0.00058, for no-gadolinium phosphor, to 0.00096 for sample with 50%Gd and then, to the highest value of 0.0028, for 75% Gd^{3+} . The minimum strain value is shown for Ce-doped $Gd_3Al_5O_{12}$, i.e. 0.00039, thus illustrating the relative higher crystalline order.

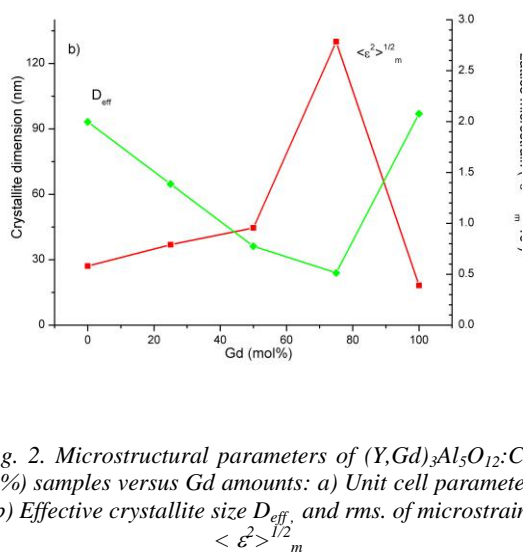
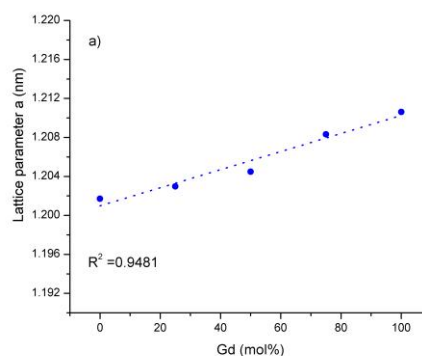


Fig. 2. Microstructural parameters of $(Y,Gd)_3Al_5O_{12} :Ce$ (1%) samples versus Gd amounts: a) Unit cell parameter; b) Effective crystallite size D_{eff} , and rms. of microstrain $\langle \varepsilon^2 \rangle_m^{1/2}$

Morphology and dimensions of phosphor particles are strongly influenced by Gd amount, as revealed by SEM investigation (Fig.3). Y-Gd-Ce-Al precursor powders consist of conglomerates of nanoparticles that disaggregate during the thermal synthesis stage, in parallel with Y-Gd-Al-hydroxide/hydrogen carbonate decomposition. Phosphor formation is a complex process "mediated" by the ammonium chloride flux that accelerates the conglomerate disaggregation, and both the formation/consolidation of yttrium gadolinium aluminium garnet and the activator incorporation. The shape and dimensions of phosphor particles seems to be extremely sensitive to gadolinium presence. As illustrates by SEM images, $Y_3Al_5O_{12} :Ce$ powder is rather homogeneous, being composed from rounded, irregular shape particles of 1-2 μm that constitute agglomerates (relatively easy to disperse). $Gd_3Al_5O_{12} :Ce$ is a homogeneous powder, formed from very regular, polyhedral particles of about 10 μm , accompanied by few, under-micron grains. $(Y,Gd)_3Al_5O_{12} :Ce^{3+}$ with 50mol% Gd is a heterogeneous material formed from regular polyhedral particles GAG:Ce type and agglomerates of 1-2 μm particles YAG:Ce type. The powder heterogeneity could probable influence the PL/PLE properties.

It appears that, gadolinium compounds from precursors behave as particle regulating agents during the

synthesis of $(Y,Gd)_3Al_5O_{12}:Ce^{3+}$ prepared by WCS-SimAdd route. The same mineralizing role of Gd^{3+} containing compounds was suggested by the continuous decrease of the temperature (T_{cryst}) of the exothermal effect that accompanies the garnet formation/crystallization (Table 1).

One can note that the precursors prepared by WCS-SimAdd route are favourable to the obtaining of $(Y,Gd)_3Al_5O_{12}:Ce^{3+}$ powders with uniform cubic crystalline structure and particle shapes and sizes convenient for optoelectronics applications. It is well known that, phosphors with spherical particles are of great importance because of their high packing density, lower scattering of light, brighter luminescent performances, and improved quality of the luminescent screen/layer promoted [16].

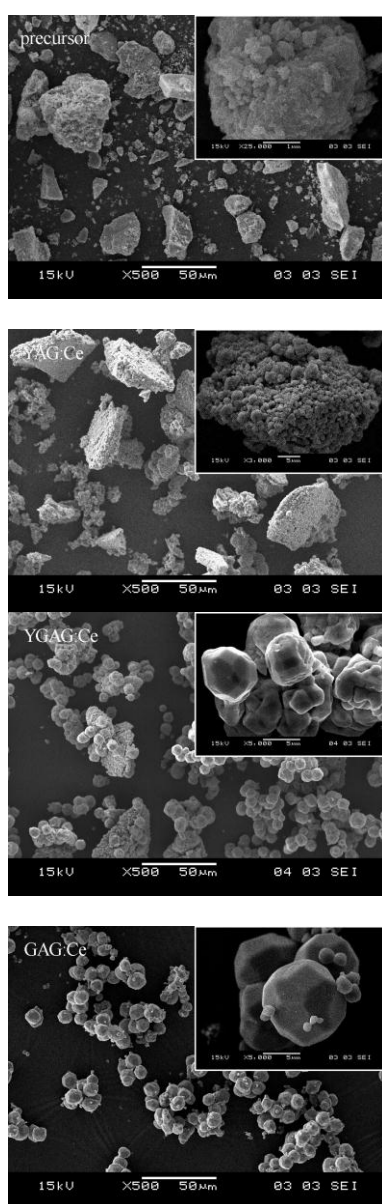


Fig. 3. SEM images of precursor and $(Y,Gd)_3Al_5O_{12}:Ce^{3+}$ (1%) phosphors with 0%, 50% and 100% Gd

3.3. Photoluminescence properties

Under ultraviolet or blue light excitation, YAG:Ce, YGAG:Ce and GAG:Ce samples show strong yellow-to-orange luminescence, in correlation with the incorporation of Ce^{3+} ions into yttrium-gadolinium aluminium garnets, with variable Gd content. The emission and excitation spectra of all samples show similar feature.

The normalized excitation (PLE) and emission (PL) spectra of the extremities of the phosphor series are depicted in Fig.4. PLE spectra of YAG:Ce and GAG:Ce contain, very weak bands at 230 and 273 nm, weak bands at about 340 nm, weak broad bands at 340 and 335 nm, and strong, fine structured bands centred at the same wavelength 452 nm, respectively. As for the PL spectra, these ones consist in one single strong emission band peaking at 530nm, and 554 nm for YAG:Ce and GAG:Ce, respectively.

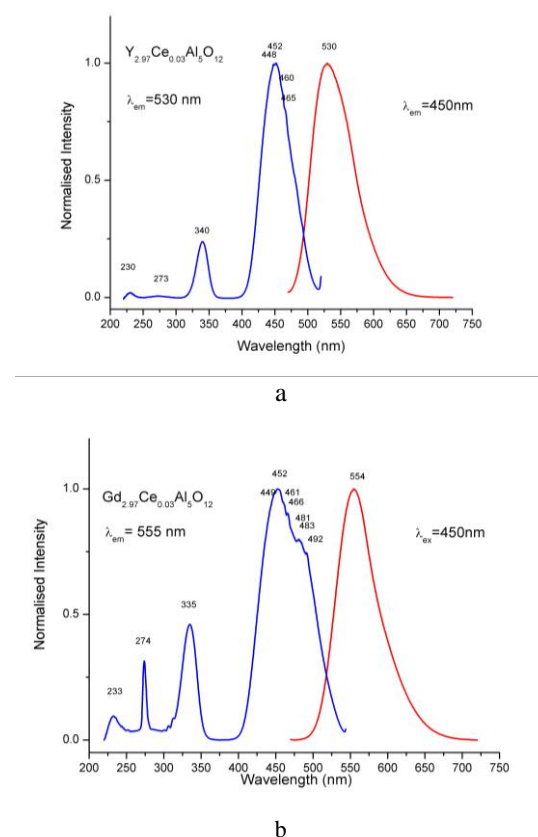


Fig.4. PLE and PL spectra of YAG:Ce (a) and GAG:Ce (b) phosphors.

PLE and PL properties of $Y_{2.97-x}Gd_x Ce_{0.03} Al_5O_{12}$ samples with variable Gd amount exhibit different spectral characteristics i.e. peak position, bandwidth (i.e. full width at half maximum FWHM) or emission intensity (band height).

PLE spectra of $Y_{2.97-x}Gd_x Ce_{0.03} Al_5O_{12}$ samples prepared with flux are depicted in Fig.5. It is obvious that, on measure that Gd amount increases, the relative middle-UV excitation band at 274 nm becomes narrower and more intense; the maximum value is attained for GAG:Ce

sample. In the same time, the near-UV band in the 300-375 nm range, increases in intensity and shifts toward shorter wavelengths (from 340 to 335 nm) with gadolinium content. As for the blue excitation band, this one becomes more and more structured and broader with gadolinium addition. For GAG:Ce sample, the integral excitation intensity in the 375-540 nm range is with about 35% higher as compared with YAG:Ce samples, whereas the bandwidth is with about 27% larger.

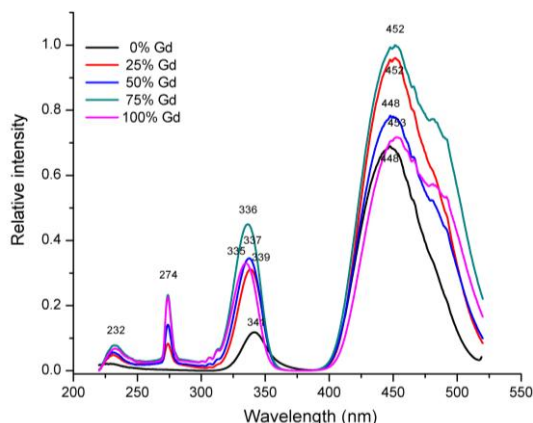


Fig. 5. PLE spectra of $(Y,Gd)_3Al_5O_{12}:Ce^{3+}$ samples prepared with variable Gd amounts (emission monitored at peak position).

The two intense broad PLE bands extended in 300-370 nm and 400-525 nm domains are due to the electronic transitions from the 4f ground state to crystal field splitting of the 5d states of Ce^{3+} ion. When the phosphors are excited by blue radiation (450 nm) the electron of Ce^{3+} ion (4f) would be raised to the higher 5d level and would be transferred afterward to the lower $^2D(5d)$ excited states. The emission of Ce^{3+} ions mainly occurs due to the transitions from $^2D(5d)$ excited states to $^2F_{7/2}(4f)$ and $^2F_{5/2}(4f)$ ground states. The PL spectra of $Y_{2.97-x}Gd_xCe_{0.03}Al_5O_{12}$ samples show a broad emission band (centred at

530-554 nm) which might be the overlapping of two emission bands associated with $^2D \rightarrow ^2F_{7/2}(4f)$ and $^2D \rightarrow ^2F_{5/2}(4f)$ transitions. These transitions of Ce^{3+} ions are due to the spin orbit coupling under the influence of Oh crystal field [16].

The spectral parameters i.e. emission intensity, peak position and bandwidth of $(Y,Gd)_3Al_5O_{12}:Ce^{3+}$ samples prepared with or without flux versus gadolinium content are depicted in Fig. 6.

For $(Y,Gd)_3Al_5O_{12}:Ce^{3+}$ prepared with ammonium chloride, the peak position and bandwidth vary monotonously with Gd amount, from 530nm to 554 nm and 73 to 63 nm, respectively. Under 450 nm excitation, a monotonous red-shift of the luminescence emission as well as a continuous narrowing of the emission band with gadolinium is observed.

The integral PL intensity varies non-monotonously with Gd concentration in $Y_{2.97-x}Gd_xCe_{0.03}Al_5O_{12}$ samples obtained in our experimental conditions. PL intensity tends to increase with gadolinium addition, the maximum values being obtained at 25 and 75 mol% Gd content. The relative small intensity observed with 50% Gd could be partially explained by the powder heterogeneity, as revealed by SEM investigation (Fig. 3). In fact, the PL performances of YAG-type phosphors are affected by the lattice native defects that could appear in the garnet structure, depending on the thermal and crystallization regime. These intrinsic defects are known to act as electron traps [19, 34].

The variation of the spectral parameters for $(Y,Gd)_3Al_5O_{12}:Ce^{3+}$ prepared with and without flux is different, thus illustrating the role of NH_4Cl in both the formation of luminescence centres and the organization/regularization of the crystalline lattice. For no-flux samples, the PL properties tend to vary non-monotonously, although the dependence curves show similar feature with the samples obtained with NH_4Cl . This support the idea that, the no-flux powders are heterogeneous luminescent materials.

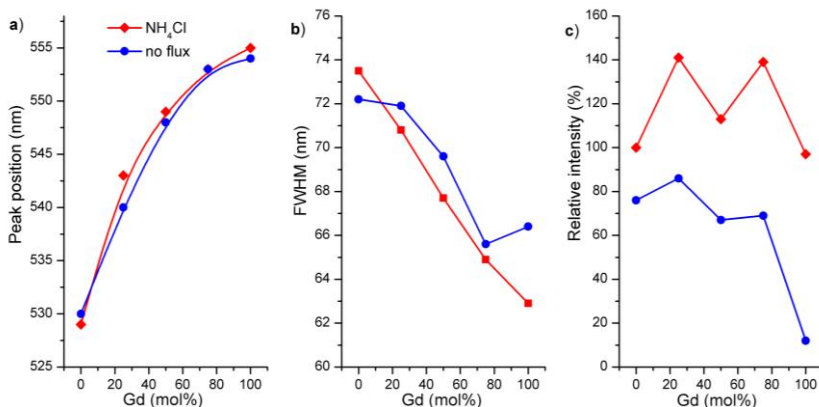


Fig.6. PL spectral characteristics for $(Y,Gd)_3Al_5O_{12}:Ce^{3+}$ versus gadolinium amount: a) Position of PL maximum; b) Full Width at Half Maximum; c) Integral PL intensity ($\lambda_{ex}=450nm$; YAG:Ce(NH_4Cl) intensity is considered 100%)

The special long wavelength of the excitation (~460 nm) and emission (~530 nm) bands of the YAG:Ce type phosphor are ascribed to the strong crystal field splitting of the 5d energy level of Ce^{3+} [35, 36]. The 5d-4f emission of Ce^{3+} depends strongly on crystal field from the garnet lowered the lowest 5d orbital energy. Usually, the Ce^{3+} emission is in the ultraviolet or blue spectral region but in $\text{Y}_3\text{Al}_5\text{O}_{12}$ garnet type lattice, it can be shifted toward longer (green-yellow) wavelength due to the influence of the crystallographic environment. As a result, the peak position and the width of the broad Ce-emission band in $(\text{Y,Gd})_3\text{Al}_5\text{O}_{12}:\text{Ce}^{3+}$ phosphors are influenced not only by Gd^{3+} amounts that substitute for Y^{3+} , but also by experimental synthesis conditions i.e. precursor quality and flux and calcination regime that both contributes to the lattice organization.

As already mentioned, it is of great significance to tune the excitation and emission bands of YAG:Ce to fit the different wavelength excitation of blue InGaN chips or to improve CRI due to the lack of a red component. Usually, with increasing the radii of the ions that substitute Y^{3+} ions from YAG:Ce, the emission of Ce^{3+} shifts to a longer wavelength. The photoluminescence of $\text{Y}_3\text{Al}_5\text{O}_{12}:\text{Ce}^{3+}$ (1mol%) sample is red-shifted with gadolinium incorporation ($r_{\text{Gd}^{3+}} = 0.108 \text{ nm}$; $r_{\text{Y}^{3+}} = 0.104 \text{ nm}$).

In order to evaluate the influence of gadolinium additions on the luminescence colour of $(\text{Y,Gd})_3\text{Al}_5\text{O}_{12}:\text{Ce}^{3+}$ phosphors, the CIE chromaticity coordinates were calculated on the basis of PL spectra registered under near-UV (345 nm) and blue-light excitation (450nm). The display of the x,y coordinates of phosphors on the chromaticity map is depicted in Fig. 7. The green-yellow-orange luminescent emission as well as the good color purity are revealed for $(\text{Y,Gd})_3\text{Al}_5\text{O}_{12}:\text{Ce}^{3+}(\text{NH}_4\text{Cl})$ samples prepared with variable Gd amount i.e. A1(0%), A2(25%), A3(50%), A4(75%) and A5(100%).

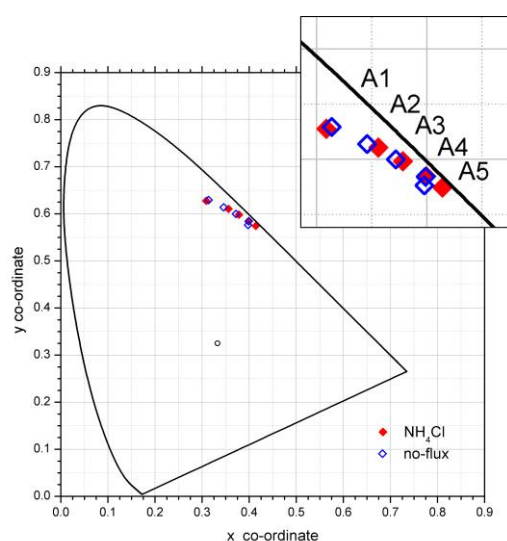


Fig. 7. $(\text{Y,Gd})_3\text{Al}_5\text{O}_{12}:\text{Ce}^{3+}$ samples displayed on the CIE chromaticity co-ordinate map (C = point of equal chromaticity)

For $(\text{Y,Gd})_3\text{Al}_5\text{O}_{12}:\text{Ce}^{3+}$ phosphors obtained with flux, gadolinium addition shifts the x, y coordinates toward both the red corner and the curve of the saturated colors of the CIE chromaticity map, regardless the excitation radiation. Similar results were obtained for no-flux samples with the mention that, in this case, in accordance with the spectral distribution curves, the x,y coordinates do not shift monotonously with Gd content. Moreover, the color purity of luminescent emission is relatively lower, as compared with flux samples.

4. Conclusions

The synthesis of cerium activated yttrium gadolinium aluminate phosphors using the wet-chemical synthesis route *via* the reagent simultaneous addition technique (WCS-SimAdd) is reported for the first time. Y-Gd-Ce-Al precursors with well defined Y:Gd ratio has been precipitated from metal nitrates and urea solutions and converted into $(\text{Y,Gd})_3\text{Al}_5\text{O}_{12}:\text{Ce}^{3+}$ phosphors with variable Gd amounts. The physical chemical characteristics of precursors and the morphological and structural as well as the photoluminescent properties of $\text{Y}_{2.97-x}\text{Gd}_x\text{Ce}_{0.03}\text{Al}_5\text{O}_{12}$ were reported, in correlation with Gd content.

WCS-SimAdd route proved to be a convenient method for the synthesis of $(\text{Y,Gd})_3\text{Al}_5\text{O}_{12}:\text{Ce}^{3+}$ type phosphors, facilitating a good control of the chemical composition and morpho-structural characteristics of precursors. The homogeneous, amorphous nanopowders of Y-Gd-Ce-Al precursors can be converted in relative mild thermal conditions into phosphors with controlled Gd content and pure cubic crystalline structure.

WCS-SimAdd route enables a good control of the synthesis conditions for yttrium gadolinium aluminium garnets with regular particle dimensions or shapes and intense yellow-to-orange emission, appropriate for use in WLED type devices.

The specific photoluminescent properties i.e. tunable spectral emission, colour purity as well as the gain in UV excitation in relation with gadolinium content recommend the as obtained $(\text{Y,Gd})_3\text{Al}_5\text{O}_{12}:\text{Ce}^{3+}$ micro-powders as luminescent materials in optoelectronics.

Acknowledgments

This work was supported by CNCSIS –UEFISCSU, project number PNII – IDEI 2488/ 2008.

References

- [1] Q. Shao, H.Li, Y.Dong, J.Jiang, C.Liang, J. He, J. Alloy. Compd. **498**, 199 (2010).
- [2] E. Fred Schubert, Light-Emitting Diodes, 2nd Edition, Cambridge University Press, Chapter 21, 2006.

- [3] P. Schlotter, J. Baur, Ch. Hielscher, M. Kunzer, H. Obloh, R. Schmidt, J. Schneider, *Mater. Sci. Eng. B* **59**, 390 (1999).
- [4] P. Schlotter, R. Schmidt, J. Schneider, *Appl. Phys. A* **64**, 417 (1997).
- [5] Y. Pan, M. Wu, Q. Su, *J. Phys. Chem. Solids* **65**, 845(2004).
- [6] H.S. Jang, W.B.Im, D.C. Lee, D.Y. Jeon, S.S. Kim, *J. Lumin.* **126**, 371 (2007).
- [7] K. Li, G. Shucai, H. Guangyan, Z. Jilin, *J. Rare Earths* **25**, 692 (2007).
- [8] Y. Pan, M. Wu, Q. Su, *Mater. Sci. Eng. B* **106**, 251(2004).
- [9] S. Lakiza, O. Fabrichnaya, Ch. Wang, M. Zinkevich, F. Aldinger, *J. Eur. Ceram. Soc.* **26**, 233 (2006).
- [10] C. Chiang, M-S.Tsai, M-H.Hon, *J. Electrochem. Soc.*, **154**, J326 (2007).
- [11] J. Li, J. Zhao, H. Zhao, J. Liang, X. Liu, B. Xu, *Spectrochim. Acta*, doi:10.1016/j.saa.2011.01.002, xxx (2011) xxx-xxx.
- [12] S. Cizauskaite, V. Reichlova, G. Nenartaviciene, A. Beganskiene, J. Pinkas, A. Kareiva, *Mater. Chem. Phys.* **102**,105 (2007).
- [13] Y. X. Pan, W. Wang, G. K. Liu, S. Skanthakumar, R. A. Rosenberg, X.Z. Guo, K. K. Li, *J. Alloy. Compd.* **488**, 638 (2009).
- [14] S. Chaudhury, S. C. Parida, K. T. Pillai, K. D. S. Mudher, *Solid State Chem.***180**, 2393 (2007).
- [15] J. Y. Park, H. C. Jung, G.S. R. Raju, B. K. Moon, J. H. Jeong, J. H. Kim, *Solid State Sci.* **12**, 719 (2010).
- [16] J. Y. Park, H. C. Jung, G.S. R. Raju, B. K. Moon, J. H. Jeong, S-M. Son, J.H. Kim, *Opt. Mater.* **32**, 293 (2009).
- [17] S. Hosokawa, Y. Tanaka, S. Iwamoto, M. Inoue, *J. Alloys Compd.* **451**, 309 (2008).
- [18] K. Zhang, W.Hu, Y. Wu, H. Liu, *Physica B*, **403**, 1678 (2008).
- [19] A. Speghini, F. Piccinelli, M. Bettinelli, *Opt. Mater.*, **33**, 247 (2011).
- [20] E.J.Popovici, L.Muresan, A. Hristea, E.Indrea, M.Vasilescu, *J.Alloy. Compd.*, **434-435**, 809 (2007).
- [21] L. Muresan, E-J. Popovici, F. Imre-Lucaci, R. Grecu, E. Indrea, *J. Alloy. Compd.* **483**, 346 (2009).
- [22] L. Muresan, E-J Popovici, R. Grecu, L. Barbu-Tudoran, *J. Alloy. Compd.* **471**, 421 (2009)
- [23] E.J.Popovici, M.Stefan, F.Imre-Lucaci, L.Muresan, E.Bica, E.Indrea, L.Barbu-Tudoran, *Physics Procedia* **2**, 603(2009). doi 10.1016/j.phpro.2009.07.046.
- [24] E.-J. Popovici, L. Muresan, M. Stefan, M. Morar, R. Grecu, E. Indrea, L. Barbu-Tudoran, *J. Optoelectron. Adv. M. - Symposia*, **2**, 136 (2010).
- [25] H. Yang, L. Yuan, G. Zhu, A. Yu, H. Xu, *Mater.Lett* **63**, 2271(2009).
- [26] J.Šubrt, V.Štengl, S.Bakardjieva, L. Szatmary, *Powder Technology* **169**, 33(2006).
- [27] J. G. Speight, *Lange's Handbook of Chemistry*, 16th ed., McGraw-Hill: New York, Section 8, 2005.
- [28] K. H. Gayer, L. C. Thompson, O. T. Zajicek, *Can. J. Chem.*, **36**, 1268(1958).
- [29] G. S. R. Raju, H. C. Jung, J. Y. Park, C. M. Kanamadi, *J. Alloy. Compds.* **481**, 730 (2009).
- [30] A. Nakatsuka, A. Yoshiasa, T. Yamanaka, *Acta Crystallogr.* **B 55**, 266 (1999).
- [31] H.M. Rietveld, *J. Appl. Cryst.* **2**, 65 (1969).
- [32] J.G.M. van Bercum, A.C. Vermeulen, R. Delhez, T.H. de Keijser, E.M. Mittemeijer, *J. Appl. Phys.* **27**, 345 (1994).
- [33] W. Kraus, G. Nolze, *J. Appl. Cryst.* **29**, 301 (1996).
- [34] C.R.Stanek, K.J.McClellan, M.R.Levy, C.Milanese, R.W.Gromes, *Nucl. Instrum. Meth. A.* **579**, 27 (2007).
- [35] G. Blasse, B.C. Grabmaier, *Luminescent Materials*, Springer Verlag, Berlin, Chapter 3, 1994.
- [36] G.Blasse, A.Bril, *J. Chem. Phys.* **47**, 5139 (1967).

*Corresponding author: jennypopovici@yahoo.com;
epopovici@chem.ubbcluj.ro